Proceedings of the 2003 IEEE/RSJ
Intl. Conference on Intelligent Robots and Systems
Las Vegas, Nevada · October 2003

Non-Redundant Robotic Manipulator Acceleration Capability and the Actuation Efficiency Measure

Alan Bowling Oussama Khatib

University of Notre Dame, Notre Dame, Indiana, USA abowling@nd.edu*
Stanford University, Stanford, California, USA khatib@cs.stanford.edu

Abstract

This article presents a performance measure, the actuation efficiency, which describes the imbalance between the end-effector accelerations achievable in different directions of non-redundant robotic manipulators. A key feature of the proposed measure is that in its development the unitary differences between linear and angular accelerations are treated in a physically meaningful manner. The measure also indicates oversized actuators, since this contributes to the imbalance in achievable accelerations. The development of this measure is based on the formulation of the Dynamic Capability Hypersurface. The shape of this hypersurface is a weak indicator of the level of imbalance in achievable end-effector accelerations.

1 Introduction

A mechanism's ability to accelerate its end-effector determines how quickly it can manipulate grasped objects, as well as its responsiveness to controller commands. This ability is referred to as *Acceleration capability* when every acceleration direction is considered. An imbalance in acceleration capability implies that the manipulator can achieve different levels of acceleration in different directions. Although a perfect balance is difficult to achieve, manipulators with a more balanced acceleration capability are versatile and adaptable, making them useful in many different tasks. Here, the *actuation efficiency* is proposed as a measure of the imbalance in acceleration capability, intended for use in manipulator design.

In this work, acceleration capability is described by the magnitude of the smallest achievable end-effector acceleration of the set of all possible accelerations from a given manipulator configuration. This magnitude is referred to as the *balanced* or *isotropic* acceleration. This quantity is useful for studying imbalances in acceleration capability, although it does not directly measure this characteristic.

*This work was completed at Stanford University.

A number of studies have examined the isotropic acceleration including [1] which presents the *Dynamic Manipulability Ellipsoid* and a method for determining the isotropic acceleration. [2] proposes condition numbers of the Jacobian and a weighted inertia tensor as measures of isotropy. [3] presents an actuator selection algorithm based on the isotropic acceleration. [4, 5] describe the *acceleration parallelepiped* from which the isotropic acceleration can be found. [6] defines the *acceleration radius*, which describes the isotropic acceleration over the workspace. [7, 8] develop *acceleration set theory* for determining the isotropic accelerations. Other studies followed the approaches listed above [9, 10].

However, these earlier studies did not address the unitary inhomogeneity between linear and angular accelerations. This limits their utility to mechanisms with three or fewer degrees-of-freedom (DOF). The unit problem was discussed extensively in [11, 12, 13, 14]. The *Dynamic Capability Hypersurface* [15] was developed to provide a description of the linear and angular balanced accelerations for a six DOF non-redundant manipulator. The proposed measure, defined as the ratio of *useful* to *available* torque, is based on the hypersurface. "Useful" torques refer to those that contribute to a balanced acceleration capability. The amount of extra available torque depends on the mechanism's dynamics and the actuator sizes. The proposed measure indicates when changes in these two areas could be beneficial.

In the next sections, a brief discussion of the balanced acceleration is presented first, followed by the development of the actuation efficiency measure. The measure is evaluated and used for the redesign of the PUMA 560 manipulator.

2 Balanced Acceleration Capability

As stated earlier, examining balanced accelerations facilitates understanding imbalances in acceleration capability. This investigation involves the relationship between the bounds on actuator torque capac-

0-7803-7860-1/03/$17.00 © 2003 IEEE

ity and end-effector acceleration, which is developed from the equations of motion,

$$A(\mathbf{q})\,\ddot{\mathbf{q}} + \mathbf{g}(\mathbf{q}) = \boldsymbol{\Gamma} = \mathsf{G}^T(\mathbf{q})\,\boldsymbol{\Upsilon}, \qquad (1)$$

the Jacobian,

$$\begin{bmatrix} v \\ \omega \end{bmatrix} = J(\mathbf{q})\,\dot{\mathbf{q}}, \qquad (2)$$

and the bounds on the actuator torque capacities,

$$-\boldsymbol{\Upsilon}_{bound} \leq \boldsymbol{\Upsilon} \leq \boldsymbol{\Upsilon}_{bound}. \qquad (3)$$

The velocity terms are omitted from equation (1) and will not be considered in this analysis. In equation (1), $\mathbf{q}$, $\mathbf{g}$, $\boldsymbol{\Gamma}$ and $\boldsymbol{\Upsilon}$ are vectors of joint/generalized coordinates, gravity forces, joint torques and actuator torques respectively. A and G are the mass matrix and the transmission matrix describing the relationship between actuator and joint torques. In equation (2), v and ω are the linear and angular end-effector velocities, and J is the Jacobian matrix. The 'dot' indicates time differentiation, for instance $\dot{v} = \frac{dv}{dt}$.

Combining equations (1) through (3) yields

$$-1 \leq E_v\dot{v} + E_\omega\dot{\omega} + N\mathsf{G}^{-T}\mathbf{g} \leq 1 \qquad (4)$$

where

$$E = [\, E_v \; E_\omega \,] = N\,\mathsf{G}^{-T}\,A\,J^{-1}. \qquad (5)$$

The reader is referred to [15] for the details. Equation (4) has been normalized by the actuator torque capacities contained in the diagonal matrix N with $N_{ii} = \frac{1}{\Upsilon_{bound_i}}$, resulting in bounds equal to one.

The balanced accelerations are determined by visualizing the terms in equation (4) as geometric objects, and exploring the relationships between them. For instance, the bounds are considered as an n-dimensional hypercube where each side has a length of two as shown in Figure 1a for a simple two DOF planar manipulator. At a particular configuration, the gravity term is constant and can be subtracted from the bounds, thereby shifting them away from the origin.

First, consider the linear balanced acceleration

$$\dot{v}^T\dot{v} = \|\dot{v}\|^2. \qquad (6)$$

It is assumed that $\|\dot{v}\|$ has some value so that equation (6) defines a sphere. The largest value of $\|\dot{v}\|$ that satisfies equation (4) is determined from the sphere's image in torque space, obtained using E_v from equation (4),

$$\boldsymbol{\Upsilon}_v^T\,(\,E_vE_v^T\,)^+\,\boldsymbol{\Upsilon}_v = \|\dot{v}\|^2 \qquad (7)$$

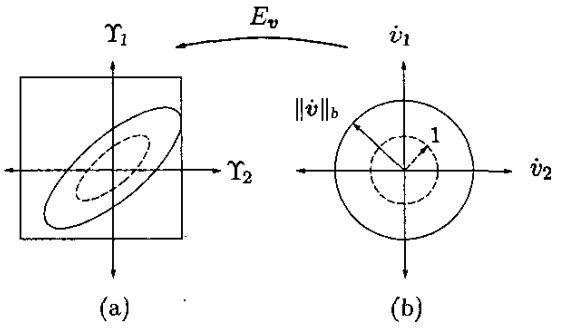

Figure 1: *Two DOF Balanced Acceleration.*

where the superscript + indicates the Moore-Penrose pseudo-inverse. This ellipsoid is mapped to the origin and expanded/contracted until it is inscribed within the torque bounds. The value of $\|\dot{v}\|$ at which this occurs determines the linear balanced acceleration $\|\dot{v}\|_b$ as shown in Figure 1.

The directions in which the ellipsoid does not touch the bounds indicate where there is more torque capacity available for achieving higher accelerations. Figure 1a shows a large imbalance in the amount of acceleration achievable in different directions. However, *it is impossible to attain a perfectly balanced acceleration capability, because the ellipsoid cannot simultaneously lie within and completely fill the volume within the torque bounds.*

A more balanced acceleration capability is obtained when the torque ellipsoid occupies as much volume within the torque bounds as possible. The ideal shape of the torque ellipsoid is not a sphere because the bounds are shifted away from the origin due to gravity. Figure 2 shows an ellipse that occupies more volume of the shifted torque bounds than the inscribed circle. The gravity shift makes portions of torque bounds unusable for producing isotropic acceleration. Note that the condition number of E_v is seldom useful for measuring the imbalance in accelerations, because it only describes the how near the ellipsoid is to a sphere.

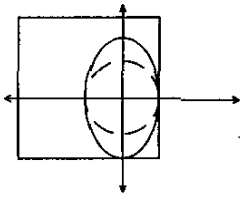

Figure 2: *Ideal Isotropy.*

Now consider both the linear and angular balanced accelerations. As in the linear case, a torque ellipsoid representing the angular balanced acceleration can

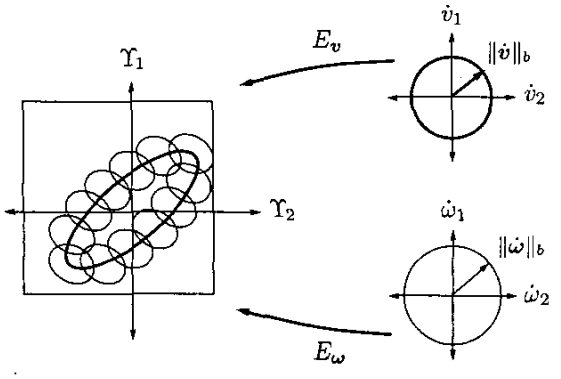

***Figure 3:** Torque Ellipse Addition.*

be developed by transforming the sphere,

$$\dot{\omega}^T\dot{\omega} \;=\; \|\dot{\omega}\|^2, \tag{8}$$

using E_ω from equation (4) into the ellipsoid,

$$\Upsilon_\omega^T \left(E_\omega E_\omega^T \right)^+ \Upsilon_\omega \;=\; \|\dot{\omega}\|^2. \tag{9}$$

The addition of the linear and angular terms in equation (4) is accomplished by mapping the center of one ellipsoid onto every point on the surface of the other, resulting in what is referred to as a *composite hypersurface*. This is valid because both ellipsoids are described in terms of torque vectors in the same space. In short, two unlike quantities are transformed into two like quantities so that they may be added. This addition is difficult to illustrate in general, so an approximation to it is shown in Figure 3.

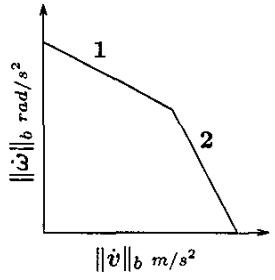

***Figure 4:** Dynamic Capability Curve.*

The composite hypersurface is expanded or contracted until it is inscribed within the bounds. However, there are many hypersurfaces which satisfy this condition. The solutions are represented by a convex, piecewise linear curve, the *Dynamic Capability Curve* shown in Figure 4. It gives the sizes of the ellipsoids in the solution set. The curve shows a tradeoff between the amount of torque used to produce linear and angular balanced accelerations. The actuator which saturated providing the level of performance along a line segment, referred to as the *limiting actuator(s)*, is indicated by a numeric label.

The Dynamic Capability Curve is described by

$$\mathbb{A}\begin{bmatrix} \|\dot{v}\| \\ \|\dot{\omega}\| \end{bmatrix} \;\leq\; \mathbb{T} \;=\; \begin{bmatrix} \mathbf{1} - N\mathrm{G}^{-T}\mathbf{g} \\ \mathbf{1} + N\mathrm{G}^{-T}\mathbf{g} \end{bmatrix} \tag{10}$$

obtained from equations (1) through (3), see [15]. Assuming that the manipulator has n actuators,

$$\begin{aligned} \mathbb{A}_{i,1} \;&=\; \mathbb{A}_{i+n,1} \;&=\; \|E_v^i\| \\ \mathbb{A}_{i,2} \;&=\; \mathbb{A}_{i+n,2} \;&=\; \|E_\omega^i\| \end{aligned} \tag{11}$$

where E_v^i indicates the i^{th} row of E_v and likewise for E_ω^i. The lines represented by each of the relations in equation (10) are overlayed in the same space, and the innermost envelope formed by them is the Dynamic Capability Curve shown in Figure 4.

3 The Actuation Efficiency Measure

The actuation efficiency, α, is based on the total volume encompassed by the union of *all* of the composite hypersurfaces described by the Dynamic Capability Curve in Figure 4, referred to as V_{useful}. For instance, this volume would resemble a cylinder for a three DOF planar manipulator. This is then divided by the volume of the torque bounds, $V_{available}$. The measure is expressed as a percentage,

$$\alpha \;=\; \frac{V_{useful}}{V_{available}}\; 100\%. \tag{12}$$

In practice, these volumes are not difficult to determine, as shown in the next sections.

3.1 Volume of Composite Hypersurfaces

The volume within the composite hypersurfaces is interpreted as the useful torque, V_{useful},

$$V_{useful.} \;=\; \int_V dV. \tag{13}$$

This integral is not difficult to evaluate because a simple cross-sectional element, the volume of one ellipsoid, can be defined. This volume is evaluated using spherical coordinates. These are $y_1 = \|\dot{\omega}\|\lambda_1 \sin(\phi)\cos(\theta)$, $y_2 = \|\dot{\omega}\|\lambda_2 \sin(\phi)\sin(\theta)$, and $y_3 = \|\dot{\omega}\|\lambda_3 \cos(\phi)$ where y_1, y_2, and y_3 are the ellipsoid's principal axes, and the λ's are the singular values of E_ω. Its volume, v_ω, is

$$\mathrm{v}_\omega(\|\dot{v}\|) \;=\; \frac{4\pi}{3}\lambda_1\lambda_2\lambda_3(m\|\dot{v}\| + c)^3 \tag{14}$$

which resembles the familiar ellipsoid volume formula, except for the radius $\|\dot{\omega}\| = m\|\dot{v}\| + c$. Recall that $\|\dot{\omega}\|$ is dependent on $\|\dot{v}\|$, as described by the Dynamic Capability Curve. The curve is piecewise linear, thus the integral is evaluated in segments.

Using equations (13) and (14), the volume obtained from a segment of the Dynamic Capability Curve, v_{useful}, is [16]

$$v_{useful} = \int\int\int v_\omega(\|\dot{v}\|)\, dx_1\, dx_2\, dx_3 \quad (15)$$

where x_1, x_2, and x_3 are orthogonal to each other and to the principal axes of the E_ω ellipsoid.

The region over which to integrate v_ω is determined by projecting the E_v ellipsoid onto x_1, x_2, and x_3. This is accomplished using the *orthogonal projector* matrix P_ω to obtain,

$$\Upsilon_x = P_\omega\, \Upsilon_v = P_\omega\, E_v\, \dot{v} \quad (16)$$
$$= \left[\, I - E_\omega E_\omega^+ \,\right] E_v\, \dot{v} \quad (17)$$

where I is the appropriately dimensioned identity matrix. Combining equations (6) and (16) yields

$$\Upsilon_x^T \left(P_\omega\, E_v\, E_v^T\, P_\omega^T \right)^+ \Upsilon_x = \|\dot{v}\|^2 \quad (18)$$

whose principal axes are x_1, x_2, and x_3. Using spherical coordinates, equation (15) becomes

$$\frac{v_{useful}}{\lambda_4\lambda_5\lambda_6} = \int_a^b \int_0^\pi \int_0^{2\pi} Z(\theta,\phi,\|\dot{v}\|)\, d\theta\, d\phi\, d\|\dot{v}\| \quad (19)$$

where

$$Z(\theta,\phi,\|\dot{v}\|) = v_\omega(\|\dot{v}\|)\|\dot{v}\|^2 \sin(\phi) \quad (20)$$

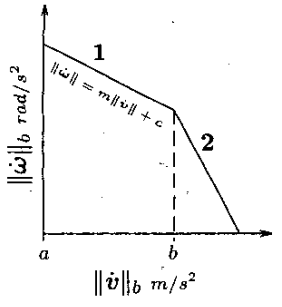

***Figure 5:** DCC.*

and where λ_4 *through* λ_6 *are the* singular values of $(P_\omega E_v)$, and a and b are the maximum and minimum values of $\|\dot{v}\|_b$ along a segment of the Dynamic Capability Curve (DCC), as shown in Figure 5.

In the six DOF case, the integrand $Z(\theta,\phi,\|\dot{v}\|)$ in equation (19) is a polynomial whose antiderivative is

$$F_{33}(\|\dot{v}\|) = \frac{8\pi^2}{3}\lambda_1\cdots\lambda_6\|\dot{v}\|^3\left(\frac{m^3}{6}\|\dot{v}\|^3 + \frac{3m^2c}{5}\|\dot{v}\|^2 + \frac{3mc^2}{4}\|\dot{v}\| + \frac{c^3}{3}\right) \quad (21)$$

where the subscript "33" denotes the dimensions of v and ω, in no particular order. In general,

$$v_{useful}(a,b) = F_{v\omega}(b) - F_{v\omega}(a), \quad (22)$$

and therefore equation (13) becomes

$$V_{useful} = \sum_{i=1}^{z} v_{useful}(a_i, b_i, c_i, m_i) \quad (23)$$

where z is the number of piecewise linear segments comprising the Dynamic Capability Curve. Note that the λ's are the singular values of E_ω and $P_\omega E_v$, $a_i \le \|\dot{v}\| \le b_i$, c_i is the $\|\dot{\omega}\|_b$-intercept, and m_i is the slope of the line segment. $F_{v\omega} = F_{\omega v}$, for mechanisms with fewer than six DOF;

$$\begin{aligned}
F_{32} &= 4\pi^2\lambda_1\cdots\lambda_5\|\dot{v}\|^3\left(\tfrac{m^2}{5}\|\dot{v}\|^2 + \tfrac{mc}{2}\|\dot{v}\| + \tfrac{c^2}{3}\right)\\
F_{31} &= 8\pi\lambda_1\cdots\lambda_4\|\dot{v}\|^3\left(\tfrac{m}{4}\|\dot{v}\| + \tfrac{c}{3}\right)\\
F_{22} &= 4\pi^2\lambda_1\cdots\lambda_4\|\dot{v}\|^2\left(\tfrac{m^2}{4}\|\dot{v}\|^2 + \tfrac{2mc}{3}\|\dot{v}\| + \tfrac{c^2}{2}\right)\\
F_{21} &= 4\pi\lambda_1\cdots\lambda_3\|\dot{v}\|^2\left(\tfrac{m}{3}\|\dot{v}\| + \tfrac{c}{2}\right).
\end{aligned} \quad (24)$$

3.2 Dynamic Capability Curve and V_{useful}

The shape of the Dynamic Capability Curve is a weak indicator of a balanced acceleration capability. The closer the curve is to forming a rectangle with the coordinate axes, as in Figure 6, the more likely a balanced acceleration capability exists at that configuration. When this occurs it means that $\|\dot{v}\|$ and $\|\dot{\omega}\|$ are independent. Thus both attain their maximum values within the bounds. This is opposed to the case when the Dynamic Capability Curve forms something closer to a triangle with the coordinate axes, as in Figure 4. The triangular shape indicates a tradeoff between $\|\dot{v}\|$ and $\|\dot{\omega}\|$; when one increases the other must decrease. This reduces the possible volume of each composite surface, and thus the manipulator should have a less balanced in acceleration capability. This is a weak indicator because α must still be calculated, since the shape of the ellipsoids, not described by the curve, must be considered.

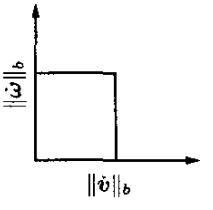

***Figure 6:** Balance Indicator.*

3.3 Inscribed Hyperellipsoid Volume

Since a perfectly balanced acceleration capability is unattainable, the unusable portions of the torque bounds are discarded from the available torque. The simplest way to do this is to use the volume, $V_{available}$, of the hyperellipsoid inscribed within the bounds, whose principal axes align with the coordinate axes. The lengths of the principal axes are determined from the gravity shifted bound vectors contained in $\mathbb{T}$, equation (10), as the element with

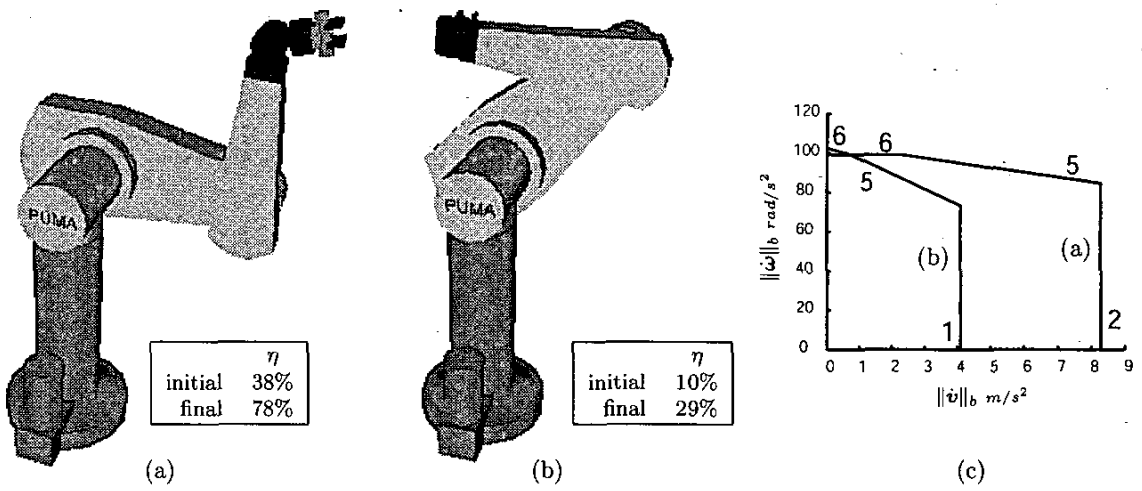

***Figure 7:** PUMA 560 Actuation Efficiencies and Dynamic Capability Curves.*

smallest absolute value for each direction. The volume of this hyperellipsoid for different dimensions is given in Table 1, where the λ's indicate the lengths of the principal axes.

$$V_{available} = d \prod_{i=1}^{n} \lambda_i$$

n	1	2	3	4	5	6
d	2	π	$\frac{4\pi}{3}$	$\frac{\pi^2}{2}$	$\frac{8\pi^2}{15}$	$\frac{\pi^3}{6}$

***Table 1:** Inscribed Hyperellipsoid Volume*

4 Application

Figures 7a and 7b show two configurations of the PUMA 560 which have different actuation efficiencies, computed for an operational point located at the intersection of the three wrist rotation axes. The model used for these computations is given in [17]. Initially the actuation efficiencies are 38% and 10%. These values indicate a large imbalance in acceleration capability.

The Dynamic Capability Curves for these two configurations, Figure 7c, tell which actuator may be suspect. Notice that for these configurations, the closer the Dynamic Capability Curve is to a rectangle, the more balanced should be the acceleration capability, as discussed in Section 3.2. The limiting actuators indicated in Figure 7c are 1, 2, 5, and 6. Therefore actuators 3 and 4 are candidates for change. The limiting actuators also suggest which motors can be changed to increase performance. Reducing the peak torque of the third actuator by half, from $1.6Nm$ to $0.8Nm$, results in new actuation efficiencies of 78% and 29%, a more than two-fold increase in acceleration capability balance for both configurations.

This actuator change neither reduces nor alters the manipulator's isotropic accelerations, given in Figure 7c. This implies that the lesser actuation efficiencies were partially due to an oversized third actuator. Recall that the shape of the ellipsoids, determined by the mechanism's dynamics, should also be considered. Reducing the size of third actuator could result in less weight for the manipulator to carry while in motion, which can lead to a better overall performance. If changing the actuators did not improve the imbalance in acceleration capability, a change in the basic mechanism design is required to achieve any improvement.

5 Conclusion

This article presented a new measure, the actuation efficiency, which describes the imbalance between the end-effector accelerations achievable in different directions. It also indicates possible actuator oversizing, since this contributes to the imbalance in acceleration capability. The measure includes both linear and angular accelerations in its description of balance in acceleration capability. This allows for the analysis of a non-redundant manipulator having up to a full six DOF. This article also establishes the shape of the Dynamic Capability Curve as a weak indicator of balance. It concludes with a design example involving the PUMA 560 manipulator. A similar

measure can be developed for force capability, which describes a manipulator's ability to apply forces and moments to the environment at the end-effector.

References

[1] Tsuneo Yoshikawa, "Dynamic manipulability of robot manipulators," in *Proceedings 1985 IEEE International Conference on Robotics and Automation*, 1985, pp. 1033–1038, St. Louis, Missouri.

[2] Kazuhiro Kosuge and Katsuhisa Furuta, "Kinematic and dynamic analysis of robot arm," in *Proceedings IEEE International Conference on Robotics and Automation*, 1985, vol. 2, pp. 1039–1044.

[3] M. Thomas, H. C. Yuan-Chou, and D. Tesar, "Optimal actuator sizing for robotic manipulators based on local dynamic criteria," *Transactions of the ASME Journal of Mechanisms, Transmissions, and Automation in Design*, vol. 107, no. 2, pp. 163–169, 1985.

[4] Oussama Khatib and Joel Burdick, "Optimization of dynamics in manipulator design: The operational space formulation," *The International Journal of Robotics and Automation*, vol. 2, no. 2, pp. 90–98, 1987.

[5] Oussama Khatib and Sunil Agrawal, "Isotropic and uniform inertial and acceleration characteristics: Issues in the design of redundant manipulators," in *Proceedings of the IUTAM/IFAC Symposium on Dynamics of Controlled Mechanical Systems*, 1989, Zurich, Switzerland.

[6] Timothy J. Graettinger and Bruce H. Krogh, "The acceleration radius: A global performance measure for robotic manipulators," *IEEE Journal of Robotics and Automation*, vol. 4, no. 1, pp. 60–69, February 1988.

[7] Yong-Yil Kim and Subhas Desa, "The definition, determination, and characterization of acceleration sets for spatial manipulators," in *The 21st Biennial Mechanisms Conference: Flexible Mechanism, Dynamics, and Robot Trajectories*, September 1990, pp. 199–205, Chicago, Illinois.

[8] Y. Kim and S. Desa, "The definition, determination, and characterization of acceleration sets for spatial manipulators," *The International Journal of Robotics Research*, vol. 12, no. 6, pp. 572–587, 1993.

[9] Ou Ma and Jorge Angeles, "The concept of dynamic isotropy and its applications to inverse kinematics and trajectory planning," in *Proceedings IEEE International Conference on Robotics and Automation*, 1990, vol. 1, pp. 481–486.

[10] Zhanfang Zhao, Zhen Wu, Jilian Lu, Weihai Chen, and Guanghua Zong, "Dynamic dexterity of redundant manipulators," in *Proceedings IEEE International Conference on Robotics and Automation*, 1995, vol. 2, pp. 928–933.

[11] H. Lipkin and J. Duffy, "Hybrid twist and wrench control for a robotic manipulator," *Journal of Mechanisms, Transmissions, and Automation in Design*, vol. 110, pp. 138–144, June 1988.

[12] Joseph Duffy, "Editorial: The fallacy of modern hybrid control theory that is based on "orthogonal complements" of twist and wrench spaces," *Journal of Robotic Systems*, vol. 7, no. 2, pp. 139–144, 1990.

[13] Keith L. Doty, Claudio Melchiorri, Eric M. Schwartz, and Claudio Bonivento, "Robot manipulability," *IEEE Transactions on Robotics and Automation*, vol. 11, no. 3, pp. 462–468, 1995.

[14] Kazem Kazerounian and Jahangir Rastegar, "Object norms: A class of coordinate and metric independent norms for displacements," *Flexible Mechanisms, Dynamics, and Analysis*, vol. 47, pp. 271–275, 1992.

[15] Alan Bowling and Oussama Khatib, "The motion isotropy hypersurface: A characterization of acceleration capability," in *Proceedings IEEE/RSJ International Conference on Intelligent Robots and Systems*, October 1998, vol. 2, pp. 965–971, Victoria, British Columbia, Canada.

[16] Jerrold E. Marsden and Anthony J. Tromba, *Vector Calculus*, John Wiley & Sons, second edition, 1976.

[17] Brian Armstrong, Oussama Khatib, and Joel Burdick, "The explicit model and inertial parameters of the puma 560 arm," in *Proceedings IEEE International Conference on Robotics and Automation*, 1986, vol. 1, pp. 510–518.